

Energy based approach for shape parameter selection in radial basis functions collocation method

Original

Energy based approach for shape parameter selection in radial basis functions collocation method / Iurlaro, Luigi; Gherlone, Marco; DI SCIUVA, Marco. - In: COMPOSITE STRUCTURES. - ISSN 0263-8223. - STAMPA. - 107:(2014), pp. 70-78. [10.1016/j.compstruct.2013.07.041]

Availability:

This version is available at: 11583/2515120 since:

Publisher:

Elsevier

Published

DOI:10.1016/j.compstruct.2013.07.041

Terms of use:

This article is made available under terms and conditions as specified in the corresponding bibliographic description in the repository

Publisher copyright

(Article begins on next page)

Energy based approach for shape parameter selection in radial basis functions collocation method

L. Iurlaro *, M. Gherlone, M. Di Sciuva

Department of Mechanical and Aerospace Engineering, Politecnico di Torino, Corso Duca degli Abruzzi, 24, 10129 Torino, Italy¹

ABSTRACT

The accuracy of the multiquadratic radial basis functions collocation method in performing elasto-static analyses of multilayer composite plates is strongly affected by the shape parameter, a value that dominates the shape of the radial basis functions. The selection of an optimal value of the shape parameter is still an open problem and several approaches have been proposed in the open literature. In this paper, a novel algorithm based on the Principle of Minimum of the Total Potential Energy is presented. The effectiveness of this algorithm is assessed by static analysis of a laminated composite plate simply supported on all edges. Comparison with other algorithms for the selection of the shape parameter is made. The radial basis functions collocation method coupled with the present algorithm results very accurate in predicting maximum deflections and stresses in the range of the span-to-thickness ratio values considered.

1. Introduction

The numerical solution of partial differential equations (PDEs) can be performed by means of two strategies: (1) the solution is approximated in each sub-domain in which the whole computational domain is divided and, successively, the solutions belonging to adjacent sub-domains are joined together along the interfaces in order to guarantee the continuity; (2) the solution derives from the overlapping of global functions, i.e. functions defined in the whole domain. Due to the feature of the former strategy, the convergence rate depends on the dimension of the sub-domains, represented by a characteristic length, raised to p th power, being p the polynomial degree of the approximation assumed in the sub-domain. On the contrary, the use of global approximation ensures an exponential convergence rate which is desirable when high accuracy has to be reached.

The finite element method [1] and the finite difference one [2] are only two examples of approximate solution techniques belonging to the first category, whereas spectral methods [3] and the radial basis function collocation method [4,5] belong to the second category. The possibility to solve PDEs in geometrically complex domains represents an important feature of a numerical technique: the finite element method, with an adequate mesh, is able to work in such geometries, whereas among all the global approximation

methods, only the radial basis functions collocation method can treat irregular domains, since no special requirements on the boundary conditions are needed. In virtue of the exponential convergence rate and the possibility to solve PDEs on complex domains, the radial basis functions collocation method has enjoyed considerable success in recent years and is increasingly applied in many fields as an alternative to the traditional solution tools.

In the structural analysis, several decades have been devoted to the development and implementation of the finite element method that has been used with great success in most practical engineering problems related to solids and structures. Although this success, in the last years some limitations that affect the finite element method become evident [6]. An investigation reveals the mesh as the main reason of these limitations. Thus, the interest towards methods not requiring any mesh, that is the so-called Meshless methods, becomes stronger.

The radial basis functions collocation method does not require a mesh to solve the PDEs but only a set of nodes arbitrarily scattered inside the domain and along its boundaries. Thus, the Meshless methods cover also the radial basis functions collocation method. According to the latter, the strong-form of the governing equations and boundary conditions are directly discretized at the field nodes using simple collocation technique to obtain a set of discretized system equations. The reader is referred to Refs. [6,7] for a detailed description.

There are different types of radial basis functions (RBF) [8] but, among these, the Hardy's multiquadratic was ranked the best in accuracy and convergence. Due to the attractive potentialities of the multiquadratic radial basis function (MQ-RBF), in [9] a deep

* Corresponding author.

E-mail addresses: luigi.iurlaro@polito.it (L. Iurlaro), marco.gherlone@polito.it (M. Gherlone), marco.disciua@polito.it (M. Di Sciuva).

¹ <http://www.polito.it>, <http://www.aesdo.polito.it>.

investigation concerning the theoretical and numerical aspects involved in the numerical solution of PDEs by means of the MQ-RBF is developed. However, despite MQ-RBF's excellent performance, it contains an user defined shape parameter, c , which affects the stability and accuracy of the solution [9]. Thus, the value of the shape parameter has to be selected carefully.

The choice of a suitable value of the shape parameter is still an open problem in research: no mathematical theory has been developed yet to rule the selection of an adequate value but several proposals are available in the open literature.

Generally speaking, three types of approaches are available: (1) models that estimate a single value of the shape parameter, assumed constant in the whole domain; (2) models that formulate a variable shape parameter strategy, i.e. compute different values of the shape parameter for each node in the domain according to an established relation or an optimization algorithm; (3) ap-proaches that bypass the problem of the optimal shape parameter selection by reducing its influence on the stability of the method.

Considering the first type of approach, the models of Fasshauer [10], Franke [11], and Hardy [12] are well known. According to them, the optimal value of the shape parameter depends only on the number of the nodes scattered in the domain, thus they provide formulas that establish such a relation. In his investigation, Rippa [13] realized that the optimal value of the shape parameter does not depend only on the number of nodes but also on several features whose effects cannot be included in a formula. Thus, an algorithm based on a statistical technique (i.e. the Leave-one-out-cross-validation, LOOCV) and able to take into account all the parameters was developed. In agreement with the Rippa' conclusions, Gherlone et al. [14] developed an algorithm for the optimal shape parameter selection based on a convergence analysis.

As stated above, the MQ-RBF collocation method experiences an exponential convergence rate according to which the accuracy of the solution improves by increasing the shape parameter [9,13,15,16]. Unfortunately, by increasing the value of the shape parameter, the problem becomes more and more ill-posed until the accuracy of the solution breaks down [9]. A way to alleviate this problem is to use a variable shape parameter strategy [9,15], that is a value of the shape parameter different from a node to another one. Following a variable shape parameter strategy, higher values of c can be used without incurring in lack of accuracy due to the ill-conditioning of the collocation matrix but this is not possible for every value of the shape parameter. In the open literature, an exponential strategy [4,5], a trigonometric [17], a linear and a random [16] one have been proposed. It is worth to note that all these variations are arbitrary and neither theoretical nor numerical considerations could suggest how the variation should be.

On the contrary, in [15] an optimization algorithm for the shape parameter selection is developed. In each node, an optimal shape parameter is computed by means of an optimization process performed by means of a genetic algorithm. The optimization tries to minimize a cost function that shows a series of local minima in the range of the shape parameter values considered, thus a genetic algorithm is required in order to catch the global minimum.

Increasing the value of the shape parameter the accuracy grows up but, at the same time, the condition number of the collocation matrix raises. The variable shape parameter strategy allows one to use, before the accuracy breaks down, values of c that are higher than those used with a constant value strategy. Nevertheless, numerical problems are only delayed. A way to definitely overcome the incurring ill-conditioning of the matrix by increasing the shape parameter, is to remove, in a certain way, the relationship between the shape parameter and the condition number of the collocation matrix. Fornberg [18] developed a strategy to pre-serve the stability and the accuracy of the solution for every value of the shape parameter used in the radial basis functions. The key

feature of his method is to consider the approximate solution, which depends on c , as a function of a complex variable, thus extending the value of the shape parameter also to the complex plane.

In the last years, several applications of the RBF collocation method in the structural analysis have been proposed. In [14,19–23] static, dynamic and stability analyses of multilayered composite and sandwich plates are performed.

Having in mind the structural applications, in the present paper a novel procedure for the shape parameter selection in radial basis function is developed. The algorithm assumes a constant value of c in the whole domain and computes it through a minimization of a cost function. It is worth to note that here, contrary to the other algorithms, the cost function is selected on the basis of physical considerations relative to the problem to be solved. Specifically, we suggest an energetically consistent approach for estimating the optimal shape parameter, i.e., an approach based on the Principle of Minimum of Total Potential Energy. In order to validate the accuracy and stability of the proposed approach, numerical results are presented and compared with the ones available in the open literature. In particular, a simply supported multilayered composite plate subjected to bi-sinusoidal transversal pressure load is analyzed using the First-order Shear Deformation Theory coupled with the radial basis functions collocation method with different choices of the optimal shape parameter. Comparisons reveal that the present algorithm ensures very accurate results, better than those estimated by means of other models.

Finally, it is worth to note that the present algorithm could be generalized to other fields once the adequate cost function that rules the problem is identified.

2. The unsymmetric radial basis functions collocation method

In this paper, the Kansa's Unsymmetric Collocation Method [4,5,19] is adopted. Consider a boundary value problem defined by

$$Du(\mathbf{x}) = s(\mathbf{x}), \text{ in } \Omega \quad (1)$$

$$Bu(\mathbf{x}) = f(\mathbf{x}), \text{ on } \partial\Omega \quad (2)$$

where Ω is the problem domain, $\partial\Omega$ its boundary, and the operators D and B are linear partial differential operators in Ω and on $\partial\Omega$, respectively. Points \mathbf{x}_i ($i = 1, \dots, N$) in Ω are identified by ($i = 1, \dots, N_I$) while those on $\partial\Omega$ by ($i = N_I + 1, \dots, N_I + N_B = N$).

The solution $u(\mathbf{x})$ may be approximated by using the following RBF-based interpolation

$$\tilde{u}(\mathbf{x}) = \sum_{i=1}^N a_i \phi_i(\|\mathbf{x} - \mathbf{x}_i\|, c) \quad (3)$$

where ϕ_i is the radial basis function (RBF) centered at \mathbf{x}_i . The RBF considered in this paper is the multiquadratic (MQ) one, which assumes the following expression

$$\phi_i(\mathbf{x}) = (\|\mathbf{x} - \mathbf{x}_i\|^2 + c^2)^{1/2} \quad (4)$$

where $\|\mathbf{x} - \mathbf{x}_i\|$ is the Euclidean norm and c the user-defined shape parameter, whose numerical value strongly influences the numerical accuracy and stability of the algorithm, as discussed in Section 2.1.

Collocation with the boundary data at the boundary points and with field equations at the interior points lead to

$$\sum_{i=1}^N a_i D\phi_i(\|\mathbf{x}_j - \mathbf{x}_i\|, c) = s(\mathbf{x}_j), \quad j = 1, \dots, N_I \quad (5)$$

$$\sum_{i=1}^N a_i B\phi_i(\|\mathbf{x}_j - \mathbf{x}_i\|, c) = f(\mathbf{x}_j), \quad j = N_I + 1, \dots, N_I + N_B \quad (6)$$

where $f(\mathbf{x}_j)$ and $s(\mathbf{x}_j)$ are the prescribed values at the boundary nodes and the function values at the interior nodes, respectively. In matrix compact form, Eqs. (5) and (6) read

$$[L]\{a\} \equiv \begin{bmatrix} D\phi \\ B\phi \end{bmatrix} \{a\} = \begin{bmatrix} s \\ f \end{bmatrix} \quad (7)$$

with an unsymmetric collocation matrix $[L]$ consisting of known coefficients. The solution of the system (7) gives the unknown vector $\{a\}$.

2.1. Methods for shape parameter selection

The accuracy of the solution of Eq. (7) and the well-conditioning of matrix $[L]$ depend on c . In a number of numerical methods that use global shape functions, such as the MQ-RBF, it has been observed [9] that, as the basis functions become flatter and flatter, the accuracy of the solution improves. This may be obtained increasing the value of c , since ϕ_i would become, in the limit, a constant function of x (see Eq. (4)). On the other hand, increasing the value of c also leads to a growth of the condition number of the matrix $[L]$ which makes the problem ill-conditioned [9]. In this situation, the round off error dominates and the solution becomes unstable; at that point, the accuracy breaks down.

Focusing on the approaches that assume a constant value of the shape parameter in the whole domain, Table 1 summarizes some of the methods proposed in the literature for the shape parameter calculation.

It is worth to note that all the models quoted in Table 1 are related exclusively with the number of nodes in the grid and with the distance between them. However, according to Rippa [13], the shape parameter should depend on many others factors, such as: the distribution of grid points, the condition number of the matrix $[L]$, the computer precision and the interpolation function, ϕ .

Motivated by these observations, Rippa [13] proposed an algorithm searching for an optimal value of the shape parameter. This algorithm minimizes a cost function that imitates the behavior of the root-mean square error between the numerical solution and the exact one. According to [13], the cost function is given by the norm of an error vector $E(c)$ with components

$$E_i(c) = \frac{a_i}{L_{ii}^{-1}} \quad (8)$$

where a_i is the i th component of the vector $\{a\}$ and L_{ii}^{-1} is the i th diagonal element of the inverse of the collocation matrix (Eq. (7)). Thus, the optimal value of the shape parameter is considered as the one which minimizes the cost function $E(c)$. Special attention must be paid to the interval inside which searching for the optimal c ; in [24] it is suggested to inspect the cost function on a large interval and then select a smaller one; this procedure is very time consuming.

Gherlone et al. [14] have recently developed an alternative algorithm for selecting the optimal value of c which takes into account all those factors considered by Rippa [13]. The approach proposed in [14] chooses the value of c that ensures the fastest rate of convergence. The rate of convergence is computed only for the control variable (in [14] the maximum displacement has been considered) and is a quantity estimated using the solution of the problem obtained with different values of c and N . For further details, see Ref. [14].

2.2. The novel algorithm for the choice of the shape parameter

The algorithm proposed in this paper is based on the Principle of the Minimum of the Total Potential Energy.

Consider a linear elastic laminated plate of uniform thickness h with N_L perfectly bonded orthotropic layers. Points of the plate are located by the orthogonal Cartesian coordinates (x, y, z) ; the

Table 1

Shape parameter selection methods. Here d represents the average distance between nodes, D is the diameter of the minimal circle enclosing all data points, while N is the number of nodes.

| Refs. | Shape parameter, c |
|----------------|----------------------|
| Fasshauer [10] | $c = 2/\sqrt{N}$ |
| Franke [11] | $c = 1.25D/\sqrt{N}$ |
| Hardy [12] | $c = 0.815d$ |

through-the-thickness coordinate is $z \in [-h/2, h/2]$, with $z = 0$ identifying the middle reference plane, or midplane, and the in-plane coordinates, (x, y) , cover the bi-dimensional space $[0, a] \times [0, b]$.

According to the First Order Shear Deformation Theory (FSDT) [25], the displacement components along the coordinate axes are expressed as

$$\begin{cases} u_x(x, y, z) = u_0(x, y) + z\phi_x(x, y) \\ u_y(x, y, z) = v_0(x, y) + z\phi_y(x, y) \\ u_z(x, y, z) = w_0(x, y) \end{cases} \quad (9)$$

here u_0 , v_0 and w_0 are the displacements of a point on the reference surface, and ϕ_x and ϕ_y are the rotations of the transverse normal about the y -axis and x -axis, respectively (see Fig. 1).

Consistent with the kinematic assumptions in Eq. (9), the FSDT accounts for transverse shear deformation, whereas the transverse normal deformations are neglected. Correspondingly, the linear in-plane and transverse shear strains are

$$\begin{aligned} \varepsilon_{xx} &= u_{0,x} + z\phi_{x,x} \\ \varepsilon_{yy} &= v_{0,y} + z\phi_{y,y} \\ \gamma_{xy} &= u_{0,y} + v_{0,x} + z(\phi_{x,y} + \phi_{y,x}) \\ \gamma_{xz} &= w_{0,x} + \phi_x \\ \gamma_{yz} &= w_{0,y} + \phi_y \end{aligned} \quad (10)$$

The generalized Hooke' law for the k th orthotropic lamina, whose principal material directions are arbitrary with respect to the midplane reference coordinates, is written as

$$\begin{Bmatrix} \sigma_{xx} \\ \sigma_{yy} \\ \tau_{xy} \\ \tau_{xz} \\ \tau_{yz} \end{Bmatrix}^{(k)} = \begin{bmatrix} Q_{11} & Q_{12} & Q_{16} & 0 & 0 \\ Q_{12} & Q_{22} & Q_{26} & 0 & 0 \\ Q_{16} & Q_{26} & Q_{66} & 0 & 0 \\ 0 & 0 & 0 & Q_{44} & Q_{45} \\ 0 & 0 & 0 & Q_{45} & Q_{55} \end{bmatrix}^{(k)} \begin{Bmatrix} \varepsilon_{xx} \\ \varepsilon_{yy} \\ \gamma_{xy} \\ \gamma_{xz} \\ \gamma_{yz} \end{Bmatrix} \quad (11)$$

where $Q_{ij}^{(k)}$ are the transformed elastic stiffness coefficients relative to the plane-stress condition that ignores the transverse-normal stress. The expressions for these coefficients in terms of the elastic moduli corresponding to the material coordinates can be found in [26].

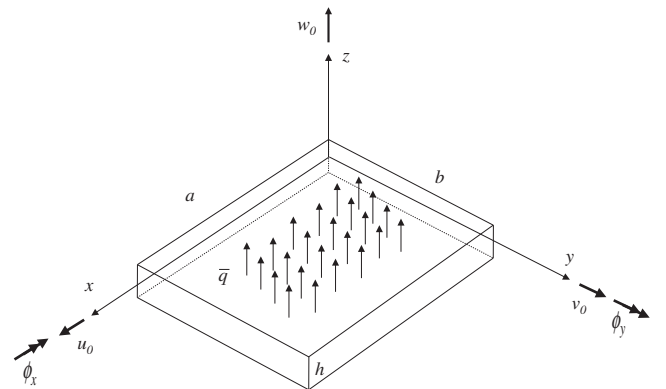


Fig. 1. Coordinate reference system, plate geometry and kinematic variables.

According to the FSDT kinematic assumptions and the definition of the linear strain tensor components (Eq. (10)), the constitutive equations relating the resultant forces and moments to the linear strain measures are

$$\begin{Bmatrix} N_x \\ N_y \\ N_{xy} \end{Bmatrix} = [A] \begin{Bmatrix} u_{0,x} \\ v_{0,y} \\ u_{0,y} + v_{0,x} \end{Bmatrix} + [B] \begin{Bmatrix} \phi_{x,x} \\ \phi_{y,y} \\ \phi_{x,y} + \phi_{y,x} \end{Bmatrix} \quad (12)$$

$$\begin{Bmatrix} M_x \\ M_y \\ M_{xy} \end{Bmatrix} = [B] \begin{Bmatrix} u_{0,x} \\ v_{0,y} \\ u_{0,y} + v_{0,x} \end{Bmatrix} + [D] \begin{Bmatrix} \phi_{x,x} \\ \phi_{y,y} \\ \phi_{x,y} + \phi_{y,x} \end{Bmatrix} \quad (13)$$

$$\begin{Bmatrix} Q_x \\ Q_y \end{Bmatrix} = k[A_T] \begin{Bmatrix} \phi_x + w_{0,x} \\ \phi_y + w_{0,y} \end{Bmatrix} \quad (14)$$

where N_x, N_{xy}, N_y are the in-plane stress resultants, Q_x, Q_y the transverse shear stress resultants, M_x, M_{xy}, M_y the bending moments, $[A], [B], [D], [A_T]$ the usual membrane, coupling, bending and transverse shear stiffness matrices, (see [26] page 128,138,139). Due to the piecewise constant through-the-thickness transverse shear strains distribution, the FSDT needs of a shear correction factor, k , necessary to take into account for the actual transverse shear stresses distribution along the thickness direction. According to the stacking sequence and the in-plane dimension, the shear correction factor in the xz -plane, k_{xz} , could be different from that in the yz -plane, k_{yz} . In the present paper, it has been assumed that $k_{xz} = k_{yz} = k$, in order to make the treatment easier. Several methods are available for computing the shear correction factors of multilayered composite and sandwich plates, readers interested to this aspect may refer to Refs. [27,28]. Moreover, a straightforward shear correction factors estimation procedure is suggested in [19].

Consider a symmetric and cross-ply laminate subjected only to a transverse pressure $\bar{q}(x,y)$; in this case, the equations governing the transverse behavior are uncoupled from those governing the in-plane behavior and read as

$$\begin{cases} D_{11} \frac{\partial^2 \phi_x}{\partial x^2} + D_{66} \frac{\partial^2 \phi_x}{\partial y^2} + (D_{12} + D_{66}) \frac{\partial^2 \phi_y}{\partial x \partial y} - kA_{44} \left(\phi_x + \frac{\partial w}{\partial x} \right) = 0 \\ D_{22} \frac{\partial^2 \phi_y}{\partial y^2} + D_{66} \frac{\partial^2 \phi_y}{\partial x^2} + (D_{12} + D_{66}) \frac{\partial^2 \phi_x}{\partial x \partial y} - kA_{55} \left(\phi_y + \frac{\partial w}{\partial y} \right) = 0 \\ kA_{44} \left(\frac{\partial \phi_x}{\partial x} + \frac{\partial^2 w}{\partial x^2} \right) + kA_{55} \left(\frac{\partial \phi_y}{\partial y} + \frac{\partial^2 w}{\partial y^2} \right) + \bar{q}(x,y) = 0 \end{cases} \quad (15)$$

The total potential energy of the plate subjected to transverse pressure $\bar{q}(x,y)$ is

$$\Pi = \frac{1}{2} \int_{-h/2}^{h/2} \int_0^a \int_0^b \{\sigma\}^T \{\varepsilon\} dx dy dz - \int_0^a \int_0^b \bar{q}(x,y) w(x,y) dx dy \quad (16)$$

where the stress and strain vectors are $\{\sigma\}^T = \{\sigma_{xx}, \sigma_{yy}, \tau_{xy}, \tau_{xz}, \tau_{yz}\}$, $\{\varepsilon\}^T = \{\varepsilon_{xx}, \varepsilon_{yy}, \gamma_{xy}, \gamma_{xz}, \gamma_{yz}\}$.

Based on FSDT, Gherlone et al. [14] presented the results, summarized in Table 2, for a simply supported multilayered composite square plate subjected to a bisinusoidal transversal pressure, comparing the solution obtained with different choices of the shape parameter in order to assess the different models present in literature. Using Eq. (16) it is possible to compute the Total Potential Energy for each solution present in Table 2 and compare the latter with that of the exact solution. The result is displayed in Table 3.

The results collected in Table 2, coupled with those of Table 3, show that the best solution, among the approximated ones, is that which reaches the minimum value of the Total Potential Energy. From this observation, it is possible to argue that a useful cost function for the shape parameter selection algorithm could be the Total Potential Energy itself, i.e., the optimal value of the shape parameter is that which ensures the minimum Total Potential Energy. Thus, as in Rippa [13] and Gherlone et al. [14], we define an

interval inside which finding the optimal value of c and, by means of an iterative procedure, for each value of c in the user defined interval, solve the boundary value problem of Eq. (7). For each solution, the Total Potential Energy is computed: when the minimum is reached, the shape parameter which corresponds to that solution is the best one in an energetic sense.

The flow chart in Fig. 2 explains the iterative procedure followed by the present algorithm.

In order to compute the total potential energy Π , the algorithm requires to perform a numerical integration: in this paper, the Gauss quadrature scheme has been applied. The domain has been divided into cells, n_q for each side; for each cell a 2×2 , 3×3 and 4×4 quadrature scheme has been used. Thus the numerical integration scheme requires defining a suitable number of quadrature cells and a right number of quadrature nodes in each cell in order to reduce the error due to numerical integration. In this way, the number of parameters that has to be selected by the user increases. In Fig. 3 there is a typical domain subdivision on quadrature cells; inside each cell a 2×2 quadrature scheme is used.

3. Static analysis of composite laminated plates using a Meshless solution approach

Let us now apply the RBF collocation method and the FSDT to the static analysis of a symmetric rectangular panel occupying the region $[0, a] \times [0, b] \times [-h/2, h/2]$. Firstly, N nodes are distributed arbitrary on the plate domain: the nodes inside the plate domain are numbered with $j = 1, \dots, N_I$ whereas the ones placed on the boundary with $j = N_I + 1, \dots, N_I + N_B = N$. The kinematic unknowns may be written as

$$\begin{Bmatrix} w \\ \phi_x \\ \phi_y \end{Bmatrix} = \sum_{i=1}^N \begin{Bmatrix} \alpha_i \\ \beta_i \\ \gamma_i \end{Bmatrix} \phi_i(\mathbf{x}) \quad (17)$$

where $\phi_i(\mathbf{x})$ represents the i th radial basis function (Eq. (4)) and $(\alpha_i, \beta_i, \gamma_i)$ are the i th kinematic unknown coefficients of the approximation. Substitution of Eq. (17) into Eqs. (15) is done for the N_I nodes inside the plate domain

$$\begin{aligned} D_{11} \sum_{i=1}^N \beta_i \phi_{i,xx}(\mathbf{x}_j) + D_{66} \sum_{i=1}^N \beta_i \phi_{i,yy}(\mathbf{x}_j) + (D_{12} + D_{66}) \sum_{i=1}^N \gamma_i \phi_{i,xy}(\mathbf{x}_j) \\ - kA_{44} \left(\sum_{i=1}^N \beta_i \phi_i(\mathbf{x}_j) + \sum_{i=1}^N \alpha_i \phi_{i,x}(\mathbf{x}_j) \right) = 0 \end{aligned} \quad (18)$$

$$\begin{aligned} D_{22} \sum_{i=1}^N \gamma_i \phi_{i,yy}(\mathbf{x}_j) + D_{66} \sum_{i=1}^N \gamma_i \phi_{i,xx}(\mathbf{x}_j) + (D_{12} + D_{66}) \sum_{i=1}^N \beta_i \phi_{i,xy}(\mathbf{x}_j) \\ - kA_{55} \left(\sum_{i=1}^N \gamma_i \phi_i(\mathbf{x}_j) + \sum_{i=1}^N \alpha_i \phi_{i,y}(\mathbf{x}_j) \right) = 0 \end{aligned} \quad (19)$$

$$\begin{aligned} kA_{44} \left(\sum_{i=1}^N \beta_i \phi_{i,x}(\mathbf{x}_j) + \sum_{i=1}^N \alpha_i \phi_{i,xx}(\mathbf{x}_j) \right) \\ + kA_{55} \left(\sum_{i=1}^N \gamma_i \phi_{i,y}(\mathbf{x}_j) + \sum_{i=1}^N \alpha_i \phi_{i,yy}(\mathbf{x}_j) \right) + \bar{q}(\mathbf{x}_j) = 0 \end{aligned} \quad (20)$$

Boundary conditions are satisfied on the N_B nodes located on the plate edges. For a rectangular plate simply supported on all edges, the boundary conditions are

$$\begin{aligned} x = 0, \quad a : w = \phi_y = M_x = 0 \\ y = 0, \quad b : w = \phi_x = M_y = 0 \end{aligned} \quad (21)$$

For example, the boundary condition on the bending moments (21) will be written as follows when using the approximation (17)

Table 2

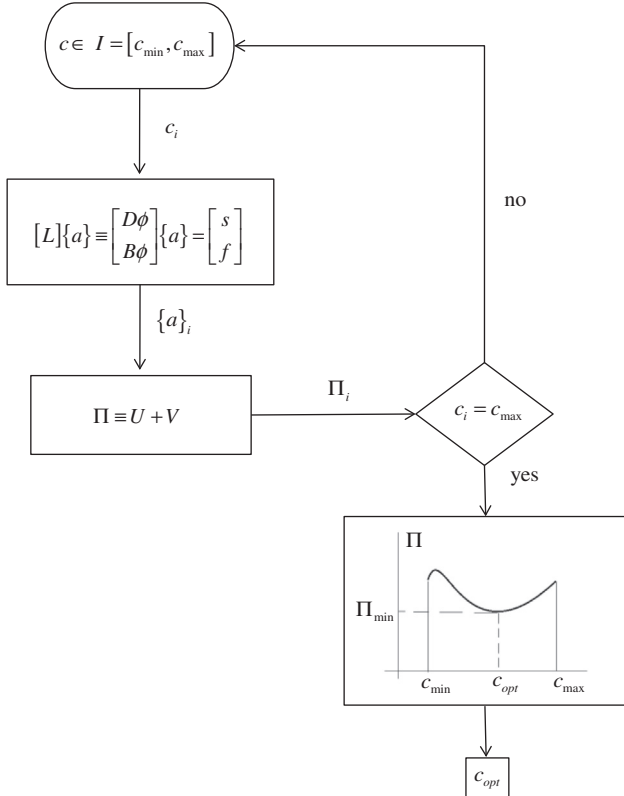
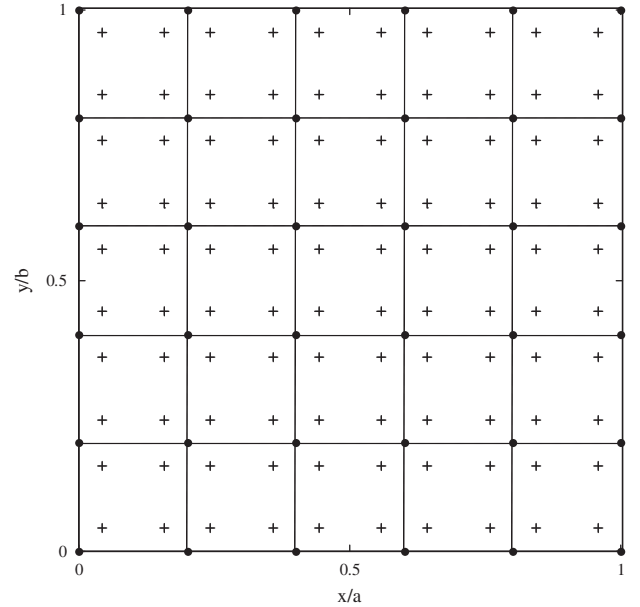
Results for a simply supported laminated composite square plate subjected to sinusoidal pressure (see [14]).

| a/h | Method | \bar{w} | $\bar{\sigma}_{xx}$ | $\bar{\sigma}_{yy}$ | $\bar{\tau}_{xz}$ | c_{opt} |
|-------|------------|-----------|---------------------|---------------------|-------------------|-----------|
| 10 | FSDT exact | 0.6628 | 0.4989 | 0.3615 | 0.3181 | |
| | RoC [14] | 0.6623 | 0.4986 | 0.3612 | 0.3056 | 0.1600 |
| | Fasshauer | 0.6651 | 0.5021 | 0.3628 | 0.3215 | 0.1168 |
| | Franke | 0.6765 | 0.5465 | 0.3688 | 1.6316 | 0.0620 |
| | Hardy | 0.6812 | 0.5310 | 0.3712 | 0.8263 | 0.0584 |
| | Rippa | 0.6620 | 0.4983 | 0.3611 | 0.3046 | 0.1699 |
| 20 | FSDT exact | 0.4912 | 0.5273 | 0.2957 | 0.3332 | |
| | RoC [14] | 0.4916 | 0.5285 | 0.2957 | 0.3245 | 0.1750 |
| | Fasshauer | 0.4986 | 0.5360 | 0.2982 | 0.3499 | 0.1168 |
| | Franke | 0.5222 | 0.5629 | 0.3082 | 0.8994 | 0.0620 |
| | Hardy | 0.5254 | 0.5668 | 0.3100 | 1.0642 | 0.0584 |
| | Rippa | 0.5158 | 0.5541 | 0.3055 | 0.2318 | 0.0723 |
| 100 | FSDT exact | 0.4337 | 0.5382 | 0.2705 | 0.3390 | |
| | RoC [14] | 0.4611 | 0.5674 | 0.2800 | 0.4458 | 0.1950 |
| | Fasshauer | 0.6032 | 0.7191 | 0.3247 | 0.7997 | 0.1168 |
| | Franke | 7.9090 | 8.8313 | 1.8805 | 9.5939 | 0.0620 |
| | Hardy | 37.8063 | 42.0710 | 7.6575 | 42.9480 | 0.0584 |
| | Rippa | 0.5246 | 0.6348 | 0.3017 | 0.6270 | 0.1406 |

Table 3

Total Potential Energy for solutions obtained with different choices of the shape parameter (Table 2).

| Method | $a/h = 10$ | $a/h = 20$ | $a/h = 100$ |
|------------|------------|------------|-------------|
| FSDT exact | 5.47e-11 | 3.20e-10 | 3.50e-08 |
| RoC [14] | 2.19e-10 | 1.29e-09 | 1.54e-07 |
| Fasshauer | 2.20e-10 | 1.31e-09 | 2.34e-07 |
| Franke | 2.30e-10 | 1.41e-09 | 3.07e-05 |
| Hardy | 2.28e-10 | 1.42e-09 | 6.38e-04 |
| Rippa | 2.19e-10 | 1.38e-09 | 1.87e-07 |

**Fig. 2.** The flow chart represents the iterative procedure. The interval I is the user-defined one inside which finding the optimal shape parameter.**Fig. 3.** Numerical integration. The dot lines represents the boundary of quadrature cells whereas the cross markers are the Gauss' quadrature points.

$$\begin{aligned}
 M_x &= D_{11} \sum_{i=1}^N \beta_i \phi_{i,x}(\mathbf{x}_j) + D_{12} \sum_{i=1}^N \gamma_i \phi_{i,y}(\mathbf{x}_j) = 0 \\
 j &= N_I + 1, \dots, N_J \quad \text{and} \quad j = N_J + 1, \dots, N_L \\
 M_y &= D_{12} \sum_{i=1}^N \beta_i \phi_{i,x}(\mathbf{x}_p) + D_{22} \sum_{i=1}^N \gamma_i \phi_{i,y}(\mathbf{x}_p) = 0 \\
 p &= N_L + 1, \dots, N_M \quad \text{and} \quad p = N_M + 1, \dots, N_N = N
 \end{aligned} \tag{22}$$

where nodes numbered from $N_I + 1$ to N_J and from $N_J + 1$ to N_L are those placed on the boundary $x = 0$ and $x = a$, respectively. In a similar manner, nodes numbered from $N_L + 1$ to N_M and from $N_M + 1$ to N_N , are those placed on the edge with $y = 0$ and $y = b$, respectively.

Table 4

Mechanical properties of unidirectional lamina.

| E_L | G_{LT} | ν_{LT} | G_{TT} |
|---------|----------|------------|----------|
| $25E_T$ | $0.5E_T$ | 0.25 | $0.2E_T$ |

Table 5

Results for a simply supported laminated composite square plate subjected to sinusoidal pressure. The interval I inside which finding the optimal shape parameter is set to be $[0.1, 0.2]$.

| a/h | Method | \bar{w} | $\bar{\sigma}_{xx}$ | $\bar{\sigma}_{yy}$ | $\bar{\tau}_{xz}$ | c_{opt} | Energy |
|-------|------------|-----------|---------------------|---------------------|-------------------|-----------|----------|
| 10 | FSDT exact | 0.6628 | 0.4989 | 0.3615 | 0.3181 | | 5.47e-11 |
| | Energy | 0.6624 | 0.4990 | 0.3614 | 0.3074 | 0.1500 | 2.19e-10 |
| | RoC [14] | 0.6623 | 0.4986 | 0.3612 | 0.3056 | 0.1600 | 2.19e-10 |
| | Fasshauer | 0.6651 | 0.5021 | 0.3628 | 0.3215 | 0.1168 | 2.20e-10 |
| | Franke | 0.6765 | 0.5465 | 0.3688 | 1.6316 | 0.0620 | 2.30e-10 |
| | Hardy | 0.6812 | 0.5310 | 0.3712 | 0.8263 | 0.0584 | 2.28e-10 |
| | Rippa | 0.6620 | 0.4983 | 0.3611 | 0.3046 | 0.1699 | 2.19e-10 |
| 20 | FSDT exact | 0.4912 | 0.5273 | 0.2957 | 0.3332 | | 3.20e-10 |
| | Energy | 0.4911 | 0.5282 | 0.2954 | 0.3238 | 0.1822 | 1.29e-09 |
| | RoC [14] | 0.4916 | 0.5285 | 0.2957 | 0.3245 | 0.1750 | 1.29e-09 |
| | Fasshauer | 0.4986 | 0.5360 | 0.2982 | 0.3499 | 0.1168 | 1.31e-09 |
| | Franke | 0.5222 | 0.5629 | 0.3082 | 0.8994 | 0.0620 | 1.41e-09 |
| | Hardy | 0.5254 | 0.5668 | 0.3100 | 1.0642 | 0.0584 | 1.42e-09 |
| | Rippa | 0.5158 | 0.5541 | 0.3055 | 0.2318 | 0.0723 | 1.38e-09 |
| 100 | FSDT exact | 0.4337 | 0.5382 | 0.2705 | 0.3390 | | 3.50e-08 |
| | Energy | 0.4586 | 0.5659 | 0.2798 | 0.4403 | 0.1979 | 1.54e-07 |
| | RoC [14] | 0.4611 | 0.5674 | 0.2800 | 0.4458 | 0.1950 | 1.54e-07 |
| | Fasshauer | 0.6032 | 0.7191 | 0.3247 | 0.7997 | 0.1168 | 2.34e-07 |
| | Franke | 7.9090 | 8.8313 | 1.8805 | 9.5939 | 0.0620 | 3.07e-05 |
| | Hardy | 37.8063 | 42.0710 | 7.6575 | 42.9480 | 0.0584 | 6.38e-04 |
| | Rippa | 0.5246 | 0.6348 | 0.3017 | 0.6270 | 0.1406 | 1.87e-07 |

Considering the $3N_I$ equilibrium Eqs. (18)–(20) together with the boundary conditions based on Eq. (21), a linear system in terms of the unknown coefficients $(\alpha_i, \beta_i, \gamma_i)$ is obtained.

4. Numerical results

In order to demonstrate the accuracy of the proposed approach in the shape parameter estimation, numerical results pertaining elasto-static deformation of multilayer laminated composite plate are presented and compared with those obtained with different choices of the shape parameter and with analytical FSDT solution.

A symmetric cross-ply composite plate, simply supported on all the edges and subjected to a bi-sinusoidal pressure, $\bar{q}(x, y) = q_0 \sin(\pi x/a) \sin(\pi y/b)$ is considered. The layers have the same thickness and the stacking sequence is $(0^\circ/90^\circ/90^\circ/0^\circ)$. Material mechanical

properties of the unidirectional lamina are reported in non-dimensional form in Table 4.

Analyses will be conducted using $k = 5/6$, although authors are conscious that this value could be not the best choice for this laminate. Because the purpose of the paper is to assess the accuracy and reliability of the algorithm for the selection of parameter c , the use of a not suitable shear correction factor is not an issue, provided that comparisons with analytical solution are made under the same conditions, in particular with the same k .

Numerical results are obtained using a 17×17 regular grid and different value of the span-to-thickness ratio, a/h .

Table 5 shows the results obtained using the present approach (FSDT solved with the MQ-RBF collocation method and the energy-based shape parameter selection algorithm, denoted as Energy) and the exact FSDT solution. Furthermore, Table 5 compares

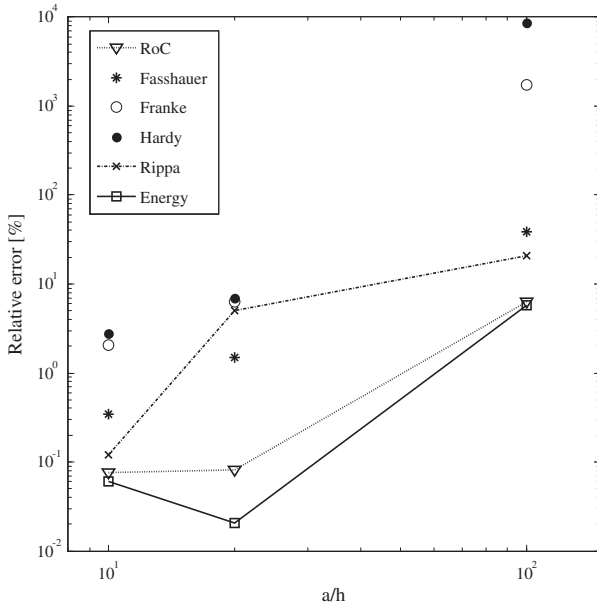


Fig. 4. Relative error on maximum displacement between the FSDT exact solution and the RBF solution with different shape parameters.

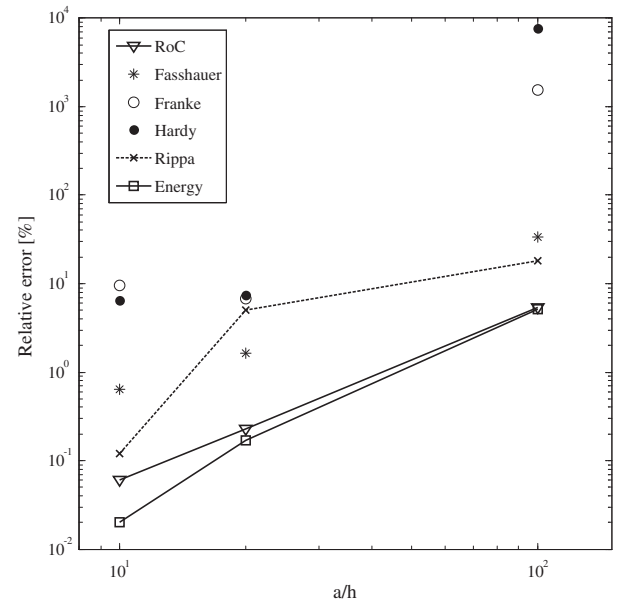


Fig. 5. Relative error on $\bar{\sigma}_{xx}$ between the FSDT exact solution and the RBF solution with different shape parameters.

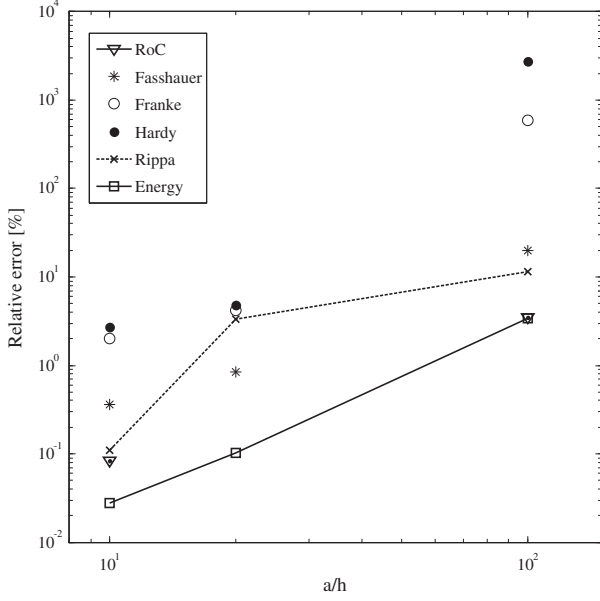


Fig. 6. Relative error on $\bar{\sigma}_{yy}$ between the FSDT exact solution and the RBF solution with different shape parameter.

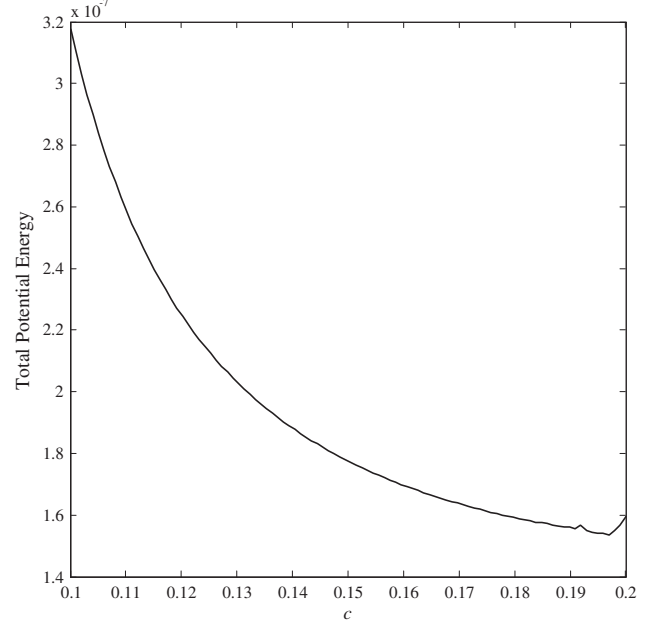


Fig. 8. Total potential energy versus shape parameter for $a/h = 100$.

solutions obtained using the MQ-RBF collocation method and the shape parameter estimated by means of the models reviewed in Section 2.1 and the algorithm presented by the authors in [14], denoted as RoC (the acronym stands for Rate of Convergence), and the one suggested by Rippa [13]. The transverse shear stresses have been estimated integrating the equilibrium equations. Stresses and displacements are given in the following non-dimensional form

$$\bar{w} = 10^2 \frac{w_{\max} h^3 E_T}{q_0 a^4} \quad \bar{\sigma}_{xx} = \frac{\sigma_{xx}(a/2, b/2, h/2) h^2}{q_0 a^2}$$

$$\bar{\sigma}_{yy} = \frac{\sigma_{yy}(a/2, b/2, h/2) h^2}{q_0 a^2} \quad \bar{\tau}_{xz} = \frac{\tau_{xz}(0, b/2, 0) h^2}{q_0 a}$$

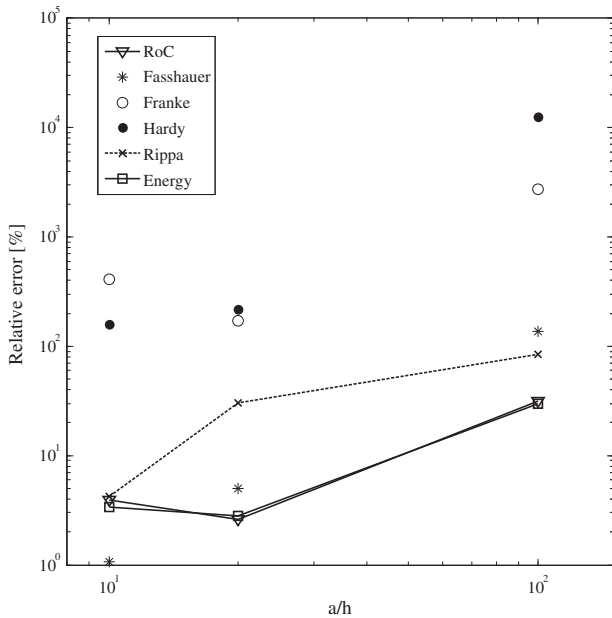


Fig. 7. Relative error on $\bar{\tau}_{xz}$ between the FSDT exact solution and the RBF solution with different shape parameters.

In order to make the comparison easier, Fig. 4 gives the log-log plot of the relative error between the maximum displacement estimated by means the FSDT exact solution and the others collected in Table 5. The same comparison, now on the stresses, is made in Figs. 5–7.

Figs. 4–7 make clear as the Energy method ensures very accurate results if compared with those obtained by means of other approaches. In Fig. 8, the trend of the Total Potential Energy versus the shape parameter is showed: the algorithm is able to catch very well the minimum of the Total Potential Energy so reaching very accurate results.

From the numerical point of view, the integration has been performed with different numbers of cells and different numbers of

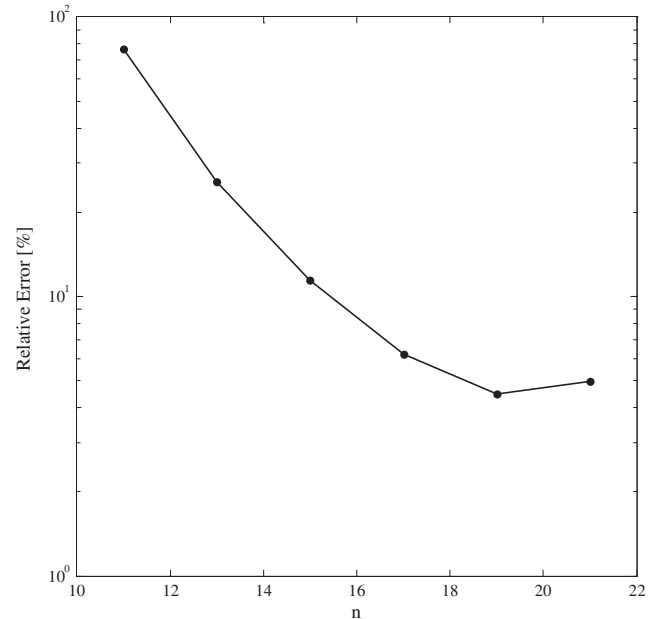


Fig. 9. Relative error versus the number of nodes along the span for the problem of laminated composite plate with span-to-thickness ratio $a/h = 100$.

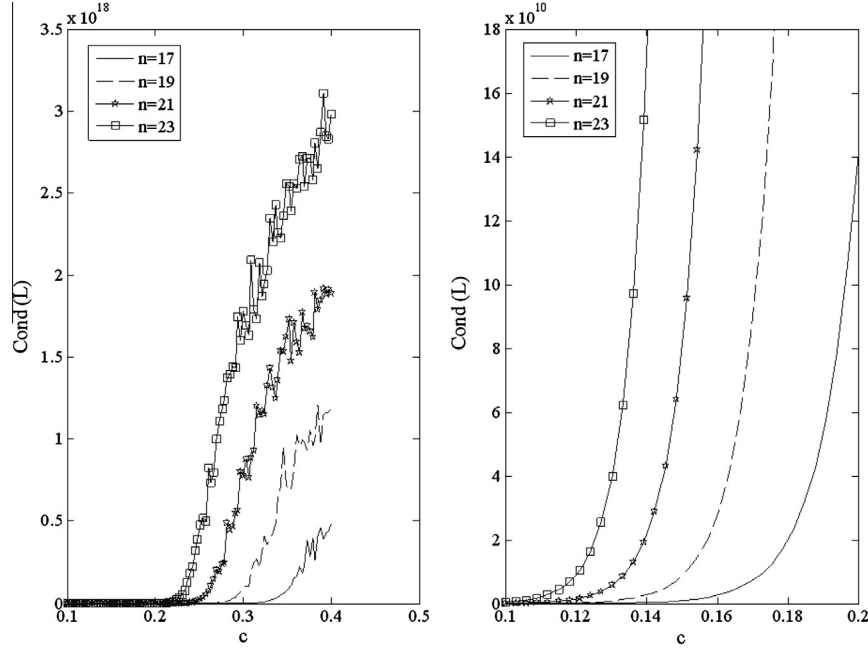


Fig. 10. Condition number of the collocation matrix for the problem of laminated composite plate with $a/h = 4$; n stands for the number of nodes along x -direction. The figure on the right is a zoomed view of figure on the left.

quadrature nodes for cell, in order to assess the convergence behavior of the method with respect to the integration parameters. From the numerical investigations performed, the results obtained with a 2×2 , 3×3 or 4×4 quadrature nodes for cell are very close to each others, while the influence of the number of quadrature cells is poor. In order to investigate the convergence behavior of the algorithm when increasing the number of nodes, in Fig. 9 the relative error on the maximum deflection computed by using the proposed algorithm with respect to the exact solution, is plotted versus the number of nodes located along the span. As it results from Fig. 9, the algorithm behaves in a convergent manner increasing the number of nodes until $n = 21$; from that point, the relative error increases if compared with that computed using $n = 19$. This could be explained by the effect of the nodes number on the condition number, as discussed below.

It is known [29] that there exists a trade-off principle according to which a high accuracy can be reached only at the cost of a low numerical stability or vice versa. This means that the use of a high value of the shape parameter leads to an accurate solution but also to a huge condition number of the collocation matrix $[L]$ of Eq. (7), causing a low numerical stability. In Fig. 10, the condition number is plotted versus the shape parameter: the relation between them is of exponential type, with the exponent depending on the number of nodes n along the x -direction of the plate (in the numerical tests performed, n is also the number of nodes along the y -direction), that is

$$\text{Cond}(L) \sim e^{\alpha(n)c}; \quad \alpha(n) \sim n \quad (23)$$

It is interesting to stress that the present algorithm is able to estimate a value of the shape parameter, in general higher than that computed by means of other algorithms, but falling in the region of numerical stability thus ensuring a solution more accurate than that reached by means of other algorithms.

5. Conclusions

The accuracy of the multiquadratic radial basis functions collocation method in predicting global and local response of multilayer

laminated composite plates is strongly affected by the shape parameter, an user-defined value that control the shape of the radial basis functions. This requires finding an optimal value of the shape parameter in order to obtain physically consistent solutions. The selection of an adequate value of the shape parameter is still an open problem in research: no mathematical theories are yet available, but several suggestions are promoted in the open literature. None of these models or algorithms focus on physical issues of the problem, but all are somehow based on mathematical or numerical aspects of the radial basis functions interpolation. Having in mind the applications to the structural problems, in this paper, a novel algorithm for the shape parameter selection in radial basis functions collocation method is suggested based on the Principle of Minimum of Total Potential Energy: the optimal value of the shape parameter is that which ensures the minimum value of the Total Potential Energy (the cost function). Contrary to the other models, the present proposal is energetically consistent, thus focusing on the physics of the problem rather than on the numerical issues.

The accuracy of the present algorithm is assessed on the problem of static deformation of rectangular, simply supported on all edges, multilayer laminated plate subjected to a bi-sinusoidal pressure. For different values of the span-to-thickness ratio, the solution obtained by means of the present algorithm is compared with those computed through other models or algorithms available in literature.

The Energy method presented in this paper appears to be very accurate ensuring better results than those obtained with other methods and sometimes also better than those estimated by means of the previous algorithm proposed by the same authors. Moreover, being linked to the physics of the problem, the present approach could be applied in other fields once the appropriate cost function that rules the problem is selected. Thus, the present algorithm does not lack of generalization.

References

- [1] Zienkiewicz OC, Taylor RL. The finite element method. The basis. Butterworth and Heinemann; 2000.

- [2] Smith GD. Numerical solution of partial differential equations: finite difference methods. 3rd ed. Oxford applied mathematics and computing science series; 1985.
- [3] Quarteroni A, Valli A. Numerical approximation of partial differential equations. Springer; 2008.
- [4] Kansa EJ. Multiquadratics – a scattered data approximation scheme with applications to computational fluid-dynamics. 1. Surface approximations and partial derivative estimates. *Comput Math Appl* 1990;19(8–9):127–45.
- [5] Kansa EJ. Multiquadratics – a scattered data approximation scheme with applications to computational fluid-dynamics. 2. Solutions to parabolic, hyperbolic and elliptic partial-differential equations. *Comput Math Appl* 1990;19(8–9):147–61.
- [6] Liu GR. Mesh free methods: moving beyond the finite element method. CRC Press; 2003.
- [7] Liu GR, Gu YT. An introduction to meshfree methods and their programming. Springer; 2005.
- [8] Power H, Barraco V. A comparison analysis between unsymmetric and symmetric radial basis function collocation methods for the numerical solution of partial differential equations. *Comput Math Appl* 2002;43:551–83.
- [9] Cheng AHD. Multiquadratic and its shape parameter – a numerical investigation of error estimate, condition number, and round-off error by arbitrary precision computation. *Eng Anal Bound Elem* 2012;36:220–39.
- [10] Fasshauer GE. Newton iteration with multiquadratics for the solution of nonlinear PDEs. *Comput Math Appl* 2002;43:4234–438.
- [11] Franke R. Scattered data interpolation tests of some methods. *Math Comput* 1982;38:181–200.
- [12] Hardy RL. Multiquadratic equations for topography and other irregular surfaces. *J Geophys Res* 1971;176:1905–15.
- [13] Rippa S. An algorithm for selecting a good value for the parameter c in radial basis function interpolation. *Advan Comput Math* 1999;11:193–210.
- [14] Gherlone M, Iurlaro L, Di Sciuva M. A novel algorithm for the shape parameter selection in radial basis functions collocation method. *Compos Struct* 2012;94:453–61.
- [15] Fornberg B, Zuev J. The Runge phenomenon and spatially variable shape parameters in RBF interpolation. *Comput Math Appl* 2007;54:379–98.
- [16] Sarra SA, Sturgill D. A random variable shape parameter strategy for radial basis function approximation methods. *Eng Anal Bound Elem* 2009;33:1239–45.
- [17] Xiang S, Wang K, Ai Y, Sha Y, Shi H. Trigonometric variable shape parameter and exponent strategy for generalized multiquadric radial basis function approximation. *Appl Math Model* 2012;36:1931–8.
- [18] Fornberg B, Wright G. Stable computation of a multiquadratic interpolants for all values of the shape parameter. *Comput Math Appl* 2004;48:853–67.
- [19] Ferreira A. Formulation of the multiquadratic radial basis function method for the analysis of laminated composite plates. *Compos Struct* 2003;59:385–92.
- [20] Ferreira AJM, Roque CMC, Martins PALS. Radial basis functions and higher-order shear deformation theories in the analysis of laminated composite beams and plates. *Compos Struct* 2004;66(1–4):287–93.
- [21] Ferreira AJM, Fasshauer GE, Batra RC, Rodrigues JD. Static deformations and vibration analysis of composite and sandwich plates using a layerwise theory and RBF-PS discretizations with optimal shape parameter. *Compos Struct* 2008;86(4):328–43.
- [22] Rodrigues JD, Roque CMC, Ferreira AJM. An improved meshless method for the static and vibration analysis of plates. *Mech Based Des Struct Mach: An Int J* 2013;41(1):21–39.
- [23] Singh S, Singh J, Shukla KK. Buckling of laminated composite plates subjected to mechanical and thermal loads using meshless collocations. *J Mech Sci Technol* 2013;27(2):327–36.
- [24] Roque CMC, Ferreira AJM. Numerical experiments on optimal shape parameters for radial basis functions. *Numer Meth Partial Different Eq* 2010;26(3):675–89.
- [25] Whitney JM, Pagano NJ. Shear deformation in heterogeneous anisotropic plates. *ASME J Appl Mech* 1970;37(4):1031–6.
- [26] Reddy JN. Mechanics of laminated composite plates and shells. CRC Press, LLC; 2004.
- [27] Vlachoutsis S. Shear correction factors for plates and shells. *Int J Numer Meth Eng* 1992;33:1537–52.
- [28] Birman V, Bert CW. On the choice of the shear correction factor in sandwich structures. *J Sand Struct Mater* 2002;4:83–95.
- [29] Ferreira AJM, Fasshauer GE. Computation of natural frequencies of shear deformable beams and plates by an RBF-pseudospectral method. *Comput Meth Appl Mech Eng* 2006;196:134–46.